ORIGINAL ARTICLE

Asian Herpetological Research 2022, 13(3): 145–158
DOI: 10.16373/j.cnki.ahr.210062

A New Brown Frog of the Genus *Rana* (Anura, Ranidae) from North China, with a Taxonomic Revision of the *R. chensinensis* Species Group

Huijun SHEN[1,2], Mengyu XU[1,2], Xinyue YANG[1,2], Zhuo CHEN[1,2*], Nengwen XIAO[3] and Xiaohong CHEN[1,2*]

[1] *College of Life Sciences, Henan Normal University, Xinxiang 453007, Henan, China*
[2] *The Observation and Research Field Station of Taihang Mountain Forest Ecosystems of Henan Province, Xinxiang 453007, Henan, China*
[3] *State Environmental Protection Key Laboratory of Regional Eco-process and Function Assessment, Chinese Research Academy of Environmental Sciences, Beijing 100012, China*

Abstract The *Rana chensinensis* species group is widely distributed throughout North China. However, its taxonomy and composition remain controversial. In recent field investigations of the Taihang Mountains, a series of *Rana* specimens were collected, which were once identified as *R. chensinensis*. However, these samples showed significant differences from *R. chensinensis* of the type locality (Shaanxi Province in the Qinling Mountains) in both morphology and genetics. In this paper, based on analyses of seventeen geographic populations from the Taihang and Qinling Mountains, we describe a new species (namely *R. taihangensis* **sp. nov.**) in the *R. chensinensis* species group. A phylogenetic analysis of the *R. chensinensis* species group based on mitochondrial genes—COI, 16S rRNA and Cytb—revealed the monophyly of the cryptic species,which formed the sister taxon to *R. kukunoris*. Morphological comparisons indicated that the cryptic species can be distinguished from its congeners by a combination of characteristics. Additionally, the distribution patterns of the *Rana* species in North China were clarified. The populations of the southwestern Taihang Mountains, Xiaoqinling Mountains, and Funiu Mountains in Henan Province remain *R. chensinensis*, whereas the populations recorded as *R. chensinensis* in Beijing City, Hebei Province, and the southeastern Taihang Mountains of Henan Province should be revised as *R. taihangensis* **sp. nov.**

Keywords morphology, phylogeny, *Rana taihangensis* **sp. nov.**, *Rana chensinensis* species group, taxonomic revision

1. Introduction

The common brown frogs (genus *Rana* Linnaeus, 1758), consisting of fifty-five known species, are widely distributed throughout Eurasia and North America, and twenty-six species among them have been found in most parts of China (Amphibia Web, 2021; Frost, 2021). However, the taxonomy and classification of this genus are still controversial. Because of the highly similar morphological features of the *Rana* species (Liu and Hu, 1961; Tanaka-Ueno *et al*., 1998; Yuan *et al*., 2016), accurate taxonomic identification and geographic delimitation are particularly difficult in the genus. Based on morphological and biogeographical data, the Chinese brown frogs were divided into the following three species groups: *R. chensinensis* species group, *R. longicrus* species group and *R. amurensis* species group (Fei *et al*., 2009). Phylogenetic analyses based on molecular data revealed more species and indicated the presence of a fourth species group—the *R. johnsi* species group (Che *et al*., 2007; Yuan *et al*., 2016; Wan *et al*., 2020). Fei *et al*. (2009) listed four species—*R. chensinensis*, *R. kukunoris*, *R. dybowskii*, and *R. asiatica*—in the *R. chensinensis* species group based on morphological similarities.

* Corresponding author: Dr. Zhuo CHEN, from Henan Normal University, Xinxiang, Henan, China, with his research focusing on systematics, phylogenetics and adaptive evolution of amphibians; Prof. Xiaohong CHEN, from Henan Normal University, Xinxiang, Henan, China, with her research focusing on the taxonomy, systematics, biogeography and evolution of amphibians.
E-mail: chenzhuo-2005@163.com (Zhuo CHEN); xhchen_xx@163.com (Xiaohong CHEN)
Received: 14 November 2021 Accepted: 20 February 2022

However, molecular evidence has suggested that *R. huanrensis* should be included in the *R. chensinensis* species group (Che *et al*., 2007; Wan *et al*., 2020), which was previously classified into the *R. amurensis* species group because of the absence of vocal sacs (Fei *et al*., 2009).

Because of the lack of morphologically diagnosable characteristics, the common brown frogs in northern China with the characteristic of a curving dorsolateral fold were all recognized as *R. chensinensis* (Li *et al*., 2014; Liu and Hu, 1996). However, a comparative analysis of morphology and karyotype regarded the populations distributed in the northeastern and northwestern China as *R. dybowskii* and *R. kukunoris*, respectively (Xie *et al*.,1999, 2000). In addition, populations from Liaoning Province, Jilin Province, and the adjacent Korean peninsula were classified as *R. huanrensis* (Amphibia Web, 2021; Frost, 2021). Thus, the *R. chensinensis* sensu stricto was mainly distributed in northern and central China, with plenty of geographic records in Beijing, Hebei, Henan, Ningxia, Shannxi, and Gansu, etc. (Fei *et al*., 2009; Frost, 2021; Qu *et al*., 1995; Wang *et al*., 1995; Wang *et al*., 2019; Wu *et al*., 2009). However, analyses of the phylogenetics and biogeography of the *R. chensinensis* species group have suggested the existence of the cryptic species in the *R. chensinensis* species group and that populations from the Loess Plateau should be an unnamed species (Zhou *et al*., 2012). It is unclear whether the possible existence of cryptic species can be revealed by morphological data and extensive sampling. In addition, the geographic distributions of the potential cryptic species and the *R. chensinensis* sensu stricto remain unresolved.

In this study, a series of *Rana* specimens were collected during the recent herpetofaunal surveys of the Taihang Mountains area in North China (Figure 1). They showed significantly morphological differences from *R. chensinensis* of the type locality (Qinling Mountains in Shaanxi Province) and were distinct from all known congeners. A molecular analysis based on three mitochondrial gene fragments—COI, 16S rRNA and Cytb—well supported the morphological differentiation and suggested the existence of a cryptic species in the *R. chensinensis* species group. Therefore, we investigated the taxonomic status of these samples and described a new species. Additionally, we proposed a taxonomic revision of the *R. chensinensis* species group in North China.

2. Materials and Methods

2.1. Sampling A total of 159 adult specimens were collected from seventeen localities of Beijing City, Hebei Province, and Henan Province throughout the Taihang Mountains (localities 1–15) and the eastern Qinling Mountains (localities 16 and 17) (Figure 1). Among them, ninety-one samples were used in a molecular analysis and 138 were measured for morphological analysis (Supplementary Table S1). All samples were kept in the Amphibian and Reptile Laboratory at Henan Normal University.

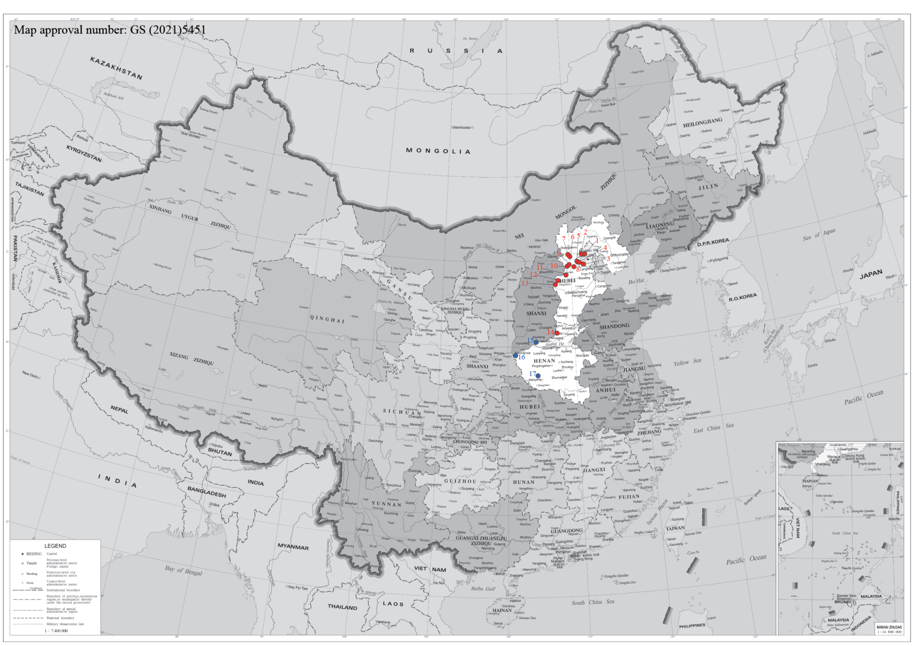

Figure 1 Distribution of sampling localities. The mtDNA subclade T and C are labeled red and blue, respectively. More locality codes and coordinates are presented in Supplementary Table S1. Map approval number: GS (2021)5451.

2.2. Laboratory protocols For comparison with the published sequence of other *Rana* species in our phylogenetic study, three partial mitochondrial DNA (mtDNA) fragments of the cytochrome c oxidase subunit I (COI), cytochrome b (Cytb), and 16S ribosomal RNA (16S rRNA) genes were amplified and sequenced. Total genomic DNA was extracted using a standard phenol-chloroform procedure (Sambrook and Russell, 2001). The primers used for polymerase chain reaction (PCR) amplifications and sequencing were summarized in Table 1. The amplification procedures followed Chen *et al.*, (2013). All new sequences were deposited in GenBank (for GenBank accession numbers see Supplementary Table S1).

2.3. Genetic diversity All nucleotide sequences were aligned using Clustal W with default parameters and checked manually in MEGA 6.0 (Tamura *et al.*, 2013). Nucleotide sites with ambiguous alignments were deleted from the analyses. Saturation tests for each gene and gene partitions were conducted using DAMBE (Xia *et al.*, 2003). The sequences from the respective samples were concatenated (Cytb + COI + 16S rRNA, 2230 bp) using SequenceMatrix v.1.8 (Vaidya *et al.*, 2011). The genetic diversity—number of polymorphic sites (S), haplotype number (h), haplotype diversity (H), and nucleotide diversity (π)—was assessed separately for Cytb, COI ,16S rRNA, and the combined sequences using DnaSP v.5.10 (Rozas *et al.*, 2003).

2.4. Phylogenetic analyses and genetic distance estimation The Bayesian inferences (BI) method was used to identify the phylogenetic relationships among the mitochondrial haplotypes of the aligned sequences. The PartitionFinder v2.1.1 (Lanfear *et al.*, 2016) was used to test the best partitioning scheme, and the jModelTest v2.1.2 was used to test the best fitting nucleotide substitution models. The best fit models for 16S rRNA was GTR + G, and that for both COI and Cytb was GTR + I + G. The BI analyses were performed in MrBayes v3.1.2 (Ronquist and Huelsenbeck, 2003), using the optimal partitioning strategy and the best-fit nucleotide substitution model for each region. The analyses were performed for 10 million generations, sampling trees every 1000 generations. The first 5000 sampled trees were discarded as burn-in, and the remaining trees were used to generate a majority-rule consensus tree and calculate the Bayesian posterior probabilities (BPP). The sequences of *Pelophylax nigromaculatus* downloaded from GenBank (for GenBank Accession numbers see Supplementary Table S1) were used as the outgroup (Che *et al.*, 2007). A phylogenetic network was computed from the distance matrix using the NeighbourNet approach implemented in SplitsTree version 4 (Huson and Bryant, 2006), using default parameters. Finally, the uncorrected p-distance model on the Cytb gene was estimated using MEGA v6.0 to evaluate the genetic divergence between *Rana* species.

2.5. Morphological analyses A total of 138 specimens (eighty-three males and fifty-five females; Supplementary Table S1) were used in the morphological study—eighty-two from the *Rana* sp., fourteen from the *R. chensinensis* species group, and forty-two from the *R. kukunoris* species group. The sex was determined by examining the pads. External measurements were made with digital calipers to the nearest 0.1 mm. Twenty-four linear measurements were the same ones presented in Shen *et al.* (2020), with the morphological description following the definition by Fei *et al.* (2009).

The morphological characteristics of the *Rana* sp. from the Taihang Mountains were compared with those of members in the *R. chensinensis* species group. Comparison characters and morphometric data of *R. chensinensis* (from its type locality, N = 15), *R. kukunoris* (N = 40), *R. dybowskii* (N = 47), and *R. huanrenensis* were taken from Fei *et al.* (2009) and voucher specimens (Supplementary Table S1).

Raw morphometric data were log-transformed for the following statistical analyses. The canonical discriminant analysis (CDA) was performed to assess the overall patterns of morphological variation among *Rana* sp., *R. chensinensis*, and *R. kukunoris* (Supplementary Table S1). One-way analysis of variance (ANOVA) was conducted to investigate the detailed interspecific variance. In the *Rana* sp., the size differences between males and females were examined by ANOVA and the analysis of covariance (ANCOVA) with snout–vent length (SVL) as covariates. The significance level was set at 0.05. These

Table 1 PCR primer information of three mitochondrial gene markers.

Locus	Primer Name	Primer Sequence	Annealing Temperature (℃)	Reference
16S	16SF	ACGAGCCTAGTGATAGCTGGTT	55	Chen *et al.*, (2013)
	16SR	CGGTCTGAACTCAGATCACGT	55	Chen *et al.*, (2013)
Cytb	HERP328	GAAAARCTRTCGTTGTWATTCAACTA	50	Yuan *et al.*, (2016)
	HERP329	CTACKGGTTGTCCYCCRATTCATGT	50	Yuan *et al.*, (2016)
COI	Chmf4	TYTCWACWAAYCAYAAAGAYATCGG	46	Che *et al.*, (2012)
	Chmr4	ACYTCRGGRTGRCCRAARAATCA	46	Che *et al.*, (2012)

analyses were carried out in R (R Development Core Team, 2010).

3. Results

3.1. Genetic diversity A total of 312 mtDNA sequences were obtained for analyses—fifty-three sequences of the Chinese *Rana* from GenBank (see Supplementary Table S1) and 259 newly obtained sequences (eighty-four for 16S rRNA, eighty-four for Cytb, and ninety-one for COI) from ninety-one individuals. The genetic diversity indexes were calculated and summarized in Table 2. A total of thirty-eight polymorphic sites and twenty-two haplotypes were detected for the 16S rRNA (966 bp) data set with a haplotype diversity of 0.874 ± 0.001 and nucleotide diversity of 0.009 ± 0.000 (Table 2). Thirty-two haplotypes (S = 53, H = 0.945 ± 0.011, π = 0.029 ± 0.001) were generated for the COI (558 bp) data set. Thirty-seven haplotypes (S = 96, H = 0.934 ± 0.000, π = 0.043 ± 0.001) were identified for the Cytb sequences. A total of fifty-two haplotypes (S = 182, H = 0.976 ± 0.008, π = 0.025 ± 0.001) were identified for the concatenated 16S rRNA + Cytb + COI data set.

3.2. Phylogenetic analyses and genetic divergence The Bayesian tree revealed four major clades (denoted Clade I–IV) with strong support: *R. chensinensis* species group, *R. amurensis* species group, *R. longicru* species group, and *R. johnsi* species group, respectively (Figure 2A). The *R. chensinensis* species group (Clade I) consisted of five highly supported lineages: subclade T, *R. kukunoris,* subclade C, *R. huanrensis*, and *R. dybowskii.* In Clade I, *Rana dybowshii* appears as the sister taxon to a clade comprising all other members of the *R. chensinensis* species group with strong support (BPP = 1.00). The well-supported subclade C (BPP = 1.00) comprised the individuals from the southwestern edge of the Taihang Mountains (locality 15) and the eastern Qinling Mountains (locality 16–17) as well as those from the type locality of *R. chensinensis.* The subclade C formed a sister-group relationship with *R. huanrensi*, but it is not well supported (BPP = 0.88). Nearly all the *Rana* samples from the Taihang Mountains (localities 1–14) were recovered as a highly supported monophyletic group (subclade T)—the sister taxon to *R. kukunoris* with strong support (BPP = 1.00). The phylogenetic network generated by SplitsTree based on the concatenated dataset was similar to the mtDNA gene tree (Figure 2B), both strongly supported the existence of a cryptic lineage in the *R. chensinensis* group.

Furthermore, the genetic divergence (uncorrected p-distance) of the Cytb gene among the studied *Rana* species is shown in Table 3. The sequence divergences within subclade T and subclade C were 1.5% and 0.2%, respectively. The mean pairwise distances between the subclade T and *R. kukunoris*, subclade T and subclade C, and subclade T and *R. chensinensis* were 4.8%, 8.4%, 8.2%, respectively. The pairwise distance among the five clades in the *R. chensinensis* species group was obviously higher than that between *R. culaiensis* and *R. zhenhaiensis* (2.5%) as well as between *R. culaiensis* and *R. longicrus* (4.4%).

3.3. Morphology The results of the one-way ANOVA and ANCOVA showed that males and females of *Rana* sp. differed in many traits, whether controlled for body size or not (Table 4). Therefore, the morphological divergence between species was examined in males and females, respectively. The canonical discriminant analysis based on twenty-four morphometric characters significantly differentiated *Rana* sp. from subclade C (i.e., *R. chensinensis*) and *R. kukunoris*—for both males and females (Figure 3). The univariate assessments by one-way ANOVA showed that both male and female *Rana* sp. were significantly different from subclade C and *R. kukunoris* in many morphometric characteristics (all $P < 0.05$; Table 4). For males, *Rana* sp. was significantly different from *R. chensinensis* in head length (HL), tympanum-eye distance (TED) and lower arm diameter (LAD) as well as different from *R. kukunoris* in snout length (SL), nostril-snout tip distance (NSD), nostril-eye length (NEL), maximum width of upper eyelid (UEW), tympanum diameter (TD), TED, LAD, hand length (HAL), tibia length (TL), and inner metatarsal tubercle width (IMTW) (all $P < 0.05$). For females, the new species differed from *R. chensinensis* in SL and TED, and it was separated from *R. kukunoris* in SL, NSD, NEL, UEW, TED, and IMTW (all $P < 0.05$).

Evidence of both molecular and morphological analyses supported the species status of *Rana* sp. (subclade T in Figure 2A) collected from Beijing City, Hebei and Henan Provinces (located in the east of the Taihang Mountains). We identified it

Table 2 The DNA polymorphism and genetic diversity based on the three mitochondrial genes of all populations.

Gene	*N*	*h*	*S*	H ± SD	π ± SD
16S (955 bp)	84	22	38	0.874 ± 0.001	0.009 ± 0.000
COI (558 bp)	84	32	53	0.945 ± 0.011	0.029 ± 0.001
Cytb (733 bp)	91	37	96	0.934 ± 0.000	0.043 ± 0.001
Aligned (2246 bp)	84	52	182	0.976 ± 0.008	0.025 ± 0.001

N: the number of individuals; *h*: the number of haplotypes; *S*: the number of polymorphic sites; H: haplotype diversity; π: nucleotide diversity; SD: standard deviation.

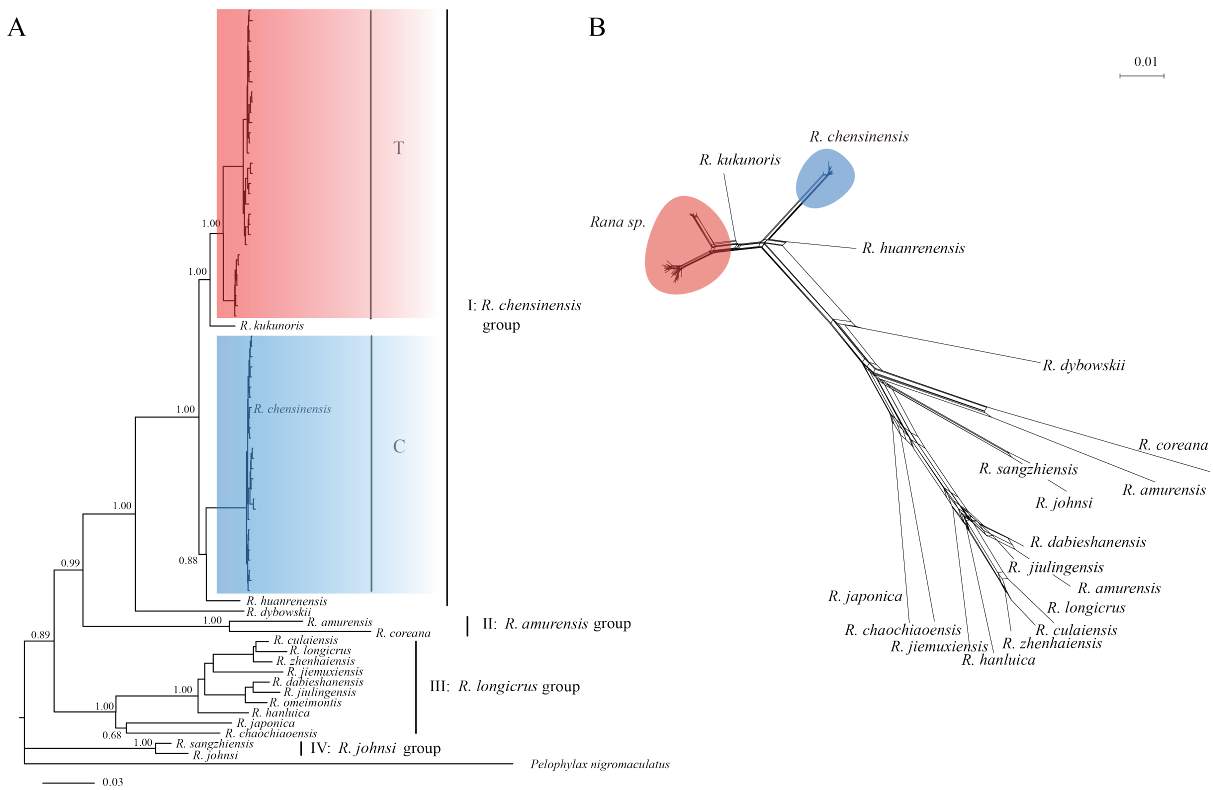

Figure 2 A: The Bayesian consensus tree inferred from the haplotypes of the combined 16S rRNA, COI, and Cytb partial sequences. Numbers near the branches represent Bayesian posterior probabilities (BPP). B: Phylogenetic network generated by SplitsTree based on the concatenated data set.

as *Rana taihangensis* Chen, **sp. nov.**

3.4. Species accounts

***Rana taihangensis* Chen, sp. nov.** (Figures 4–9; Table 5)

Holotype HNNU2104II018, an adult male (Figures 4A, B, E; 5A, B), was collected by M.Y. Xu and Y. J. Zhu on April 9, 2021, from Huixian City (35°37′43.60″N, 113°36′24.84″E, 1025 m a. s. l.) in Henan Province, China.

Allotype HNNU2104II019, an adult female (Figures 4C, D, E; 5C, D), was collected with the holotype (HNNU2104II018).

Paratypes Eighty adult specimens (52 males, 28 females) from the Taihang Mountain area in Beijing City, Hebei and Henan Provinces were collected by X. H. Chen, M. Y. Xu, X. Y. Yang, Y. Q. Lu, Q. Q. Feng, D. Liu, C. Ke, Y. M. Zhang, S. X. Gao, Y. J. Zhu, Y. Liu, G. L. Hu, W. K. He and T. H. Wang during 2003 and 2021(Supplementary Table S1). All the type specimens were deposited in the Herpetological Research Laboratory, College of Life Science, Henan Normal University.

Etymology The specific name taihangensis is in reference to the type localities in Beijing City, Hebei and Henan Provinces of the Taihang Mountains, North China.

Diagnosis *Rana taihangensis* **sp. nov.** differs from its congeners by the following combination of characteristics: (1) body medium-sized, SVL = 37.06–55.42 (44.87 ± 4.03, N = 52) mm in adult males, 38.41–63.30 (46.96 ± 6.02, N = 28) mm in adult females; (2) snout obtusely rounded, canthus rostralis obtuse and raised prominently; (3) interorbital distance (IOD) less than internarial distance (IND) and the width of upper eyelid (UEW); (4) tympanum diameter equal (TD) less than half of the eye diameter; (5) vomerine teeth in two short oblique series, anterior edges suited in the posterior border of the choanae; (6) supratympanic fold extending from the eye to over the shoulder; (7) dorsolateral fold narrow, extending from the posterior canthus to crotch, slight curving above the tympanic membrane; (8) dorsal and ventral skin smooth; (9) the color of the dorsal surface changing with environment from reddish-brown, light pink-orange, light brown, grayish-white to olive patterns; (10) dorsum of limbs with black-brown transverse bars; (11) dorsum of limbs with black-brown transverse bars; (12) heels overlapping when hindlimbs flexed at right angles to axis of body; (13) fingers unwebbed, relative finger lengths: III>I>IV>II; (14) toes two-thirds webbed, relative toe lengths: IV>V≈III>II>I; (15) internal subgular vocal sacs and red lineae musculinae present in males; (16) nuptial pad dark brown, developed into two groups with an obvious gap on the ventral

Table 3 The pairwise uncorrected p-distance (%) of the Cytb partial sequence (733 bp) used in this study.

	1	2	3	4	5	6	7	8	9	10	11	12	13	14	15	16	17	18
1	**0.015**																	
2	0.084	**0.002**																
3	0.082	0.001																
4	0.048	0.069	0.068															
5	0.081	0.063	0.062	0.060														
6	0.130	0.128	0.128	0.106	0.114													
7	0.182	0.189	0.188	0.179	0.207	0.181												
8	0.173	0.167	0.166	0.175	0.186	0.172	0.050											
9	0.184	0.177	0.177	0.171	0.197	0.174	0.044	0.025										
10	0.178	0.180	0.179	0.173	0.190	0.170	0.111	0.105	0.106									
11	0.175	0.174	0.174	0.168	0.168	0.165	0.101	0.090	0.084	0.101								
12	0.180	0.184	0.184	0.178	0.187	0.188	0.103	0.095	0.088	0.107	0.041							
13	0.174	0.177	0.176	0.174	0.185	0.180	0.087	0.084	0.085	0.093	0.087	0.080						
14	0.167	0.152	0.152	0.156	0.171	0.179	0.158	0.147	0.147	0.158	0.156	0.165	0.135					
15	0.169	0.167	0.167	0.156	0.175	0.163	0.167	0.133	0.139	0.143	0.150	0.153	0.141	0.146				
16	0.189	0.187	0.187	0.192	0.203	0.190	0.220	0.208	0.208	0.187	0.181	0.169	0.183	0.200	0.200			
17	0.201	0.195	0.195	0.193	0.214	0.202	0.207	0.202	0.196	0.198	0.203	0.198	0.184	0.204	0.207	0.154		
18	0.190	0.178	0.178	0.180	0.206	0.178	0.180	0.171	0.175	0.182	0.175	0.188	0.191	0.192	0.177	0.204	0.219	
19	0.227	0.215	0.214	0.215	0.224	0.223	0.198	0.190	0.186	0.198	0.194	0.213	0.206	0.220	0.213	0.216	0.203	0.204

Note: bold values indicate intraspecies distance. 1: Clade T, 2: Clade C, 3: *R. chensinensis*, 4: *R. kukunoris*, 5: *R. huanrenensis*, 6: *R. dybowskii*, 7: *R. longicrus*, 8: *R. zhenhaiensis*, 9: *R. culaiensis*, 10: *R. jiemuxiensis*, 11: *R. dabieshanensis*, 12: *R. omeimontis*, 13: *R. hanluica*, 14: *R. chaochiaoensis*, 15: *R. japonica*, 16: *R. amurensis*, 17: *R. coreana*, 18: *R. johnsi*.

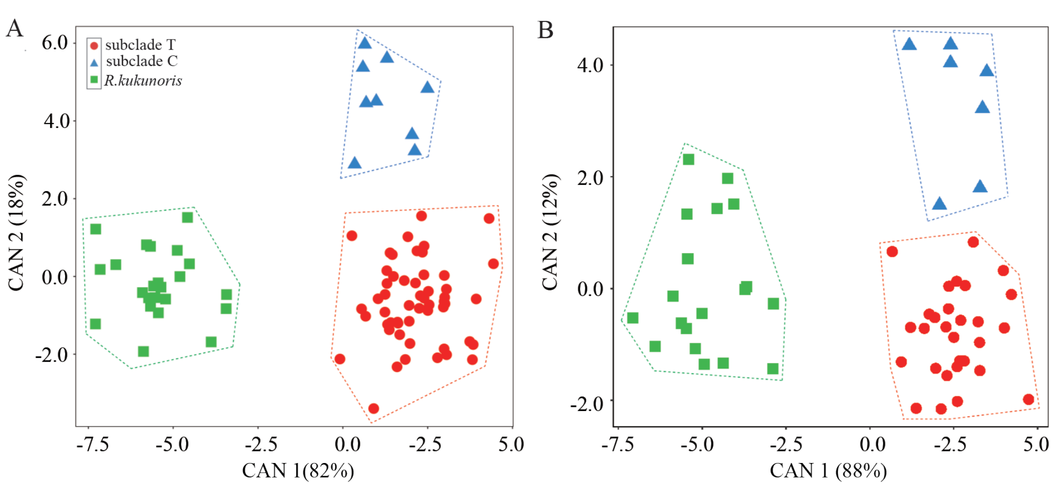

Figure 3 Results of canonical discriminant analysis of samples representing subclade T, subclade C and *R. kukunoris* in males (A) and females (B), respectively. Different lineages or species are denoted with different colors and shapes.

side of finger I in males; and (17) fertilized eggs dark brown with grayish brown poles, mean diameter of 1.9 mm.

Description of holotype SVL 47.31 mm. Head slightly longer than broad (HL/HW = 1.06), snout obtusely rounded in dorsal view, projecting beyond the lower lip; canthus rostralis obtuse and raised prominently; nostril closer to tip of snout than eye; loreal region concave, sloping outwards; interorbital distance (IOD) less than internarial distance (IND) and the width

Table 4 *P* values of one-way ANOVA (applied to log-transformed original data) and ANCOVA (using SVL as covariates) for morphometric comparisons between the sexes and between species in *R. taihangensis* **sp. nov.**, *R. chensinensis* and *R. kukunoris*.

	Males vs. Females in RT		In males		In females	
	Size-corrected	Original	RT vs. RC	RT vs. RK	RT vs. RC	RT vs. RK
SVL		0.087 F	0.477	0.200	0.304	0.478
HL	**<0.001***F**	0.052 F	**0.021***	0.924	0.609	0.880
HW	**<0.001***F**	0.058 F	0.258	0.254	0.250	0.744
SL	**<0.001***F**	**0.012 *F**	0.749	**0.002****	**0.045***	**0.014***
NSD	**0.034*F**	0.068 F	0.264	**0.008****	0.060	**0.003****
NEL	**<0.001***F**	**0.008 **F**	0.489	**<0.001*****	0.209	**<0.001*****
IND	**0.003**F**	**0.028 *F**	0.259	0.975	0.403	0.464
IOD	0.079 F	0.107 F	0.380	0.057	0.998	0.920
IFE	**<0.001***F**	**0.027 *F**	0.484	**0.030***	0.071	0.162
IAE	**<0.001***F**	**0.026 *F**	0.973	0.855	0.221	0.410
ED	**0.019*M**	0.114 F	1.000	0.489	0.975	0.671
UEW	0.142 F	0.275 F	0.522	**<0.001*****	0.782	**<0.001*****
TD	0.255 M	0.421 F	0.257	**<0.001*****	0.358	0.106
TED	**0.004**F**	**0.002**F**	**<0.001*****	**0.002****	**0.001****	**<0.001*****
LAHL	0.065 M	0.418 M	0.974	0.257	0.548	0.997
LAD	**<0.001***M**	**<0.001***M**	**<0.001*****	**<0.001*****	0.169	**0.001****
HAL	0.174M	0.553 F	0.717	**0.044***	0.299	0.316
HLL	**0.001***M**	0.277 F	0.967	0.437	0.410	0.137
TL	**<0.001***M**	0.230 F	0.980	**0.021***	0.434	0.075
TW	0.622 M	0.807 F	0.368	0.423	0.167	0.297
FTL	0.105 M	0.704 F	0.978	0.875	0.376	0.377
FL	0.955 M	0.941 F	0.906	0.987	0.814	0.732
OMTL	**0.021*F**	**0.050 *F**	0.317	0.998	0.921	1.000
IMTW	0.542 M	0.847 F	0.307	**<0.001*****	0.872	**<0.001*****

Note: RT, RC and RK represent *R. taihangensis* **sp. nov.**, *R. chensinensis* and *R. kukunoris* in respective. Significant statistics were shown as bold values (significant level is 0.05; *: $P < 0.05$; **: $P < 0.01$; ***: $P < 0.001$). Letters followed by values present the larger sex. F: females; M: males.

of upper eyelid (UEW); tympanum diameter shorter than half of eye diameter (TD/ED = 0.47); tongue deeply notched posteriorly; vomerine teeth in two short oblique series, anterior edges suited in the posterior border of choanae (Figure 4A, B).

Forelimbs: Forearm robust, length of lower arm and hand less than half of SVL (LAHL/SVL = 0.45); relative finger lengths: III>IV>I>II; fingers slender, without web nor narrow fringe; one prominent subarticular tubercle on fingers I and II, two tubercle on fingers III and IV; prominent supernumerary tubercles below the base of fingers III and IV; inner metacarpal tubercle ovoid, two outer metacarpal tubercles distinctly separated, slightly larger, long elliptic; dark brown nuptial pad on the ventral side of finger I, without spines, clearly divided into two parts, the larger one close to the tip of finger I extending beyond the supernumerary tubercles, the basal one smaller (Figures 4B; 5A).

Hindlimbs: Hindlimbs 171% of SVL, tibio-tarsal articulation reaching to the anterior corner of eyes when leg stretched forward; foot length and tibia length larger than half of SVL; heels overlapping when the limbs are held at right angles to body axis; the relative toe lengths: IV>V≈III>II>I; toe tips rounded, unexpanded, with narrow fringes; subarticular tubercles small and distinct with two tubercles on toes I and II, three tubercle on toes III and V, four on toe IV; inner metatarsal tubercle large, ovoid, outer small, round; toes two-thirds webbed, reaching the base of the disk, except toe IV webbed to the distal subarticular tubercle (Figures 4A, B; 5A, B).

Skin rather smooth, irregular tubercles sparsely scattered on dorsum surface; several small tubercles on flank; supratympanic fold well developed and extending from the eyes to over the shoulder; a triangular brown patch behind the eyes and anterior to the temporal fold; dorsolateral fold distinct and thin,

Figure 4 A–B: Dorsal and ventral views of the holotype (HNNU2104II018, male); C–D: Dorsolateral and ventral views of the allotype (HNNU2104II019, female); E: Dorsolateral view of the amplexus of the holotype (upper) and allotype (lower); F: Eggs of female *R. taihangensis* **sp. nov.**

Figure 5 Ventral views of the left hand (A) and foot (B) of the holotype in life (HNNU2104II018, male). Ventral views of the right hand (C) and the left foot (D) of the allotype (HNNU2104II019, female).

extending from the posterior canthus to crotch, slight curving above the tympanic membrane; a mass of grannules on throat and belly, tiny whitish grannules around vent.

Coloration in life Dorsal side reddish brown with blurred dark brown spots; on dorsum a x-shaped elongated tubercle with blurred dark blots, reaching posterior of upper eyelid; lip

greyish brown with light yellow spots; a black spot in front of each nostril; dorsolateral fold light reddish; nuptial pad dark brown; color of forelimbs and hindlimbs light reddish; four faint brown bars in the forearm, five clear brown bars in both thigh and tibia; throat and chest creamy white, belly greyish white; ventral side of hands, limbs, and foot webbing reddish; metacarpal tubercles, distal subarticular tubercle, supernumerary tubercles and foot webbing red; grannules on throat and belly yellowish or whitish; light yellowish markings on throat; light reddish markings on chest; yellowish mottled markings on belly.

Coloration in preservative Dorsal side grayish brown, tubercles on dorsum light reddish, dorsolateral fold and upper eyelid light reddish brown; nuptial pad black; strips on limbs brown; venter dark gray, dark brown spots on throat; ventral surface of hindlimbs light reddish brown; metacarpal tubercles, distal subarticular tubercle and supernumerary tubercles reddish brown.

Variation in the type series The variations in morphometric measurements of the type series from fourteen populations across its distribution range are listed in Table 5. The type series exhibit high intraspecific variation in color and spot patterns (Figure 6). The dorsal surface is greyish white in male HNNU2104I006 (Figure 6A), light pinkish orange in female HNNU2104I004 and male HNNU2104I008 (Figure 6C, D), and greenish brown in male HNNU20TI06057 (Figure 6E). Although black spots are present on the dorsum in most specimens, HNNU2104II008 and HNNU20TI06033 lack spots on the dorsum (Figure 6D, F). In 119 adult male specimens, the number of nuptial pads on finger I is two in most males (72%, Figure 6G); moreover, some individuals have another one (19%) or two (9%) small, unclear nuptial pads on the tips of their fingers (Figure 6H, I).

Sexual dimorphism The body size of the females (SVL, mean 44.87 ± 4.03 mm, *N* = 28) is slightly smaller than that of the males (SVL, mean 46.72 ± 6.16 mm, *N* = 52). Females are significantly larger than males in HL, head width (HW), SL, NSD, NEL, internarial distance (IND), distance between

Table 5 Morphometric measurements (in mm) of the type series of *R. taihangensis* **sp. nov.** with mean ± SD (range) and ratio of each measurement to the SVL (%).

Traits	Holotype	Males (*N* = 52)		Allotype	Females (*N* = 28)	
		Mean ± SD (range)	%		Mean ± SD (range)	%
SVL	47.31	44.87 ± 4.03 (37.06–55.42)	–	49.48	46.96 ± 6.02 (38.41–63.30)	–
HL	14.27	14.78 ± 1.01 (12.41–16.91)	32.94	16.40	15.46 ± 1.94 (12.13–21.07)	32.92%
HW	13.46	14.25 ± 1.27 (12.04–17.58)	31.76	15.67	15.01 ± 2.21(12.11–22.03)	31.97%
SL	7.09	6.69 ± 0.57 (5.63–7.95)	14.91	7.45	7.08 ± 0.75 (5.60–9.12)	15.08%
NSD	2.76	3.08 ± 0.31 (2.42–3.88)	6.86	3.18	3.21 ± 0.36 (2.44–4.23)	6.84%
NEL	3.98	3.41 ± 0.32 (2.62–4.02)	7.59	3.21	3.65 ± 0.43 (2.98–4.85)	7.77%
IND	3.43	3.70 ± 0.33 (2.92–4.38)	8.24	4.18	3.89 ± 0.46 (3.13–4.94)	8.29%
IOD	2.27	2.46 ± 0.34 (1.52–3.23)	5.49	2.39	2.59 ± 0.37 (2.05–3.66)	5.51%
IFE	6.75	6.44 ± 0.53 (5.38–7.56)	14.35	6.62	6.82 ± 0.90 (4.96–9.45)	14.52%
IAE	10.96	10.13 ± 0.79 (8.56–12.21)	22.57	10.75	10.64 ± 1.17 (9.20–13.65)	22.67%
ED	6.10	5.93 ± 0.55 (4.99–7.28)	13.21	5.89	6.15 ± 0.67 (4.98–7.50)	13.10%
UEW	3.39	3.56 ± 0.37 (2.76–4.35)	7.93	3.75	3.66 ± 0.44 (3.03–4.58)	7.79%
TD	2.89	2.85 ± 0.35 (2.11–3.87)	6.35	2.66	2.92 ± 0.40 (2.29–3.95)	6.22%
TED	1.04	1.44 ± 0.27 (0.95–2.12)	3.20	1.35	1.601 ± 0.23 (1.24–2.25)	3.41%
LAHL	21.29	20.93 ± 1.78 (16.66–25.15)	46.65	21.18	20.63 ± 2.58 (17.02–26.35)	43.93%
LAD	5.01	3.59 ± 0.60 (2.34–5.22)	8.01	3.23	3.10 ± 0.68 (2.24–5.37)	6.59%
HAL	11.80	11.51 ± 1.03 (9.29–14.84)	25.64	12.29	11.70 ± 1.36 (9.75–14.40)	24.91%
HLL	81.06	76.09 ± 7.47 (64.32–96.23)	169.59	83.34	78.48 ± 9.88 (63.91–102.34)	167.12%
TL	24.35	23.32 ± 2.23 (18.83–28.44)	51.97	25.91	24.16 ± 3.25 (19.21–31.89)	51.45%
TW	5.02	4.80 ± 0.71 (2.75–6.92)	10.69	4.57	4.87 ± 0.94 (3.60–8.03)	10.37%
FTL	37.48	34.73 ± 3.36 (28.58–42.77)	77.39	36.87	35.20 ± 4.40 (29.22–46.71)	74.95%
FL	26.89	24.90 ± 2.53 (20.47–31.44)	55.50	26.47	24.94 ± 3.09 (21.31–34.24)	53.11%
OMTL	2.03	2.25 ± 0.33 (1.65–3.13)	5.01	2.46	2.39 ± 0.31 (1.85–3.10)	5.08%
IMTW	0.80	0.88 ± 0.15 (0.54–1.36)	1.95	1.21	0.90 ± 0.23 (0.40–1.57)	1.91%

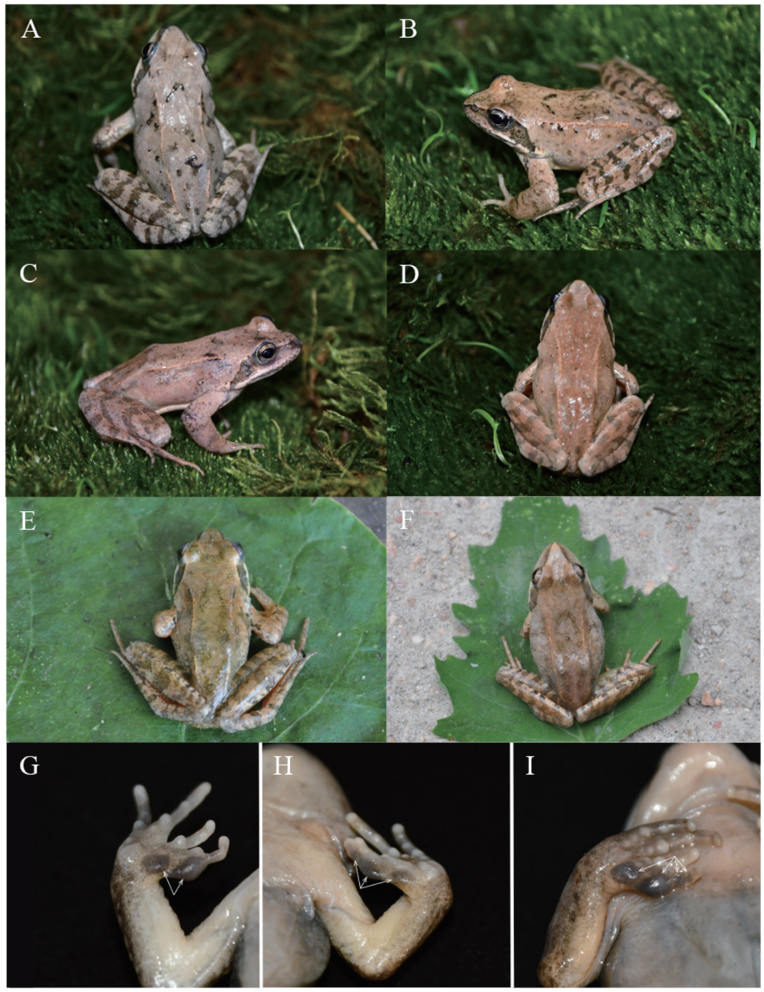

Figure 6 Variation of color patterns in living *R. taihangensis* **sp. nov.** Dorsal view of HNNU2104II006 (male; A); dorsolateral view of HNNU2104II003 (male; B), dorsolateral view of HNNU2104II004 (male; C); and dorsal view of HNNU2104II008 (female; D) from the type locality, Huixian City, Henan Province, China. E: Dorsal view of HNNU20TI06057 (male) from Fuping County, Hebei Province, China. F: Dorsal view of HNNU20TI06033 (female) from Pingshan County, Hebei Province, China. G–I: The varied number of nuptial pads from two to four in HNNU20TI08012 from Yixian County and HNNU1907VI028 and HNNU1907VI034 from Huailai County, Hebei Province, China.

anterior corner of eyes (IFE), distance between posterior corner of eyes (IAE), TED, and outer metatarsal tubercle length (OMTL) (all $P < 0.05$, Table 5). The males are significantly larger than the females in LAD, length of hind leg (HLL), and TL (all $P < 0.01$, Table 5).

Distribution and ecology *Rana taihangensis* **sp. nov.** is known from the east slope of the Taihang mountain area in Beijing City, Hebei Province, and Henan Province. All specimens were found around water pools or slow streams at 116–1 943 m elevations surrounded by shrubs and small hardwoods (Figure 7). At the type locality, Huixian City of Henan Province (113.61°E, 35.63°N, 1 073m a.s.l), females began to spawn on April 6, and amplexus pairs could be found as late as on April 24. Adult females spawn 331–707 eggs (N = 6, mean 483) at one time with a mean diameter of 1.9 mm (N = 7, range 1.7–2.0 mm). The fertilized eggs are dark brown with grayish brown poles (Figure 4F). The breeding season was approximately from early to late April. The tadpoles are yellowish-brown on the dorsal side (Figure 8A, B), with tail fins lightly colored and small golden spots scattered on the whole body. At the Gosner stage 25, the average total length (TOL) is 13.26 mm, and the tail is 144% of SVL. At the thirty-fifth stage the average TOL is 28.21 mm, and the tail is 232% of SVL. The dorsal fin arises behind the origin of the tail. The tail muscles are strong, and the tip of the tail is blunt. The nostrils are near snout, and the eyes are positioned dorsally (Figure 8A, B). The keratodont row formula

Figure 7 Typical habitat of *R. taihangensis* **sp. nov.** in Huixian City, Henan Province, China.

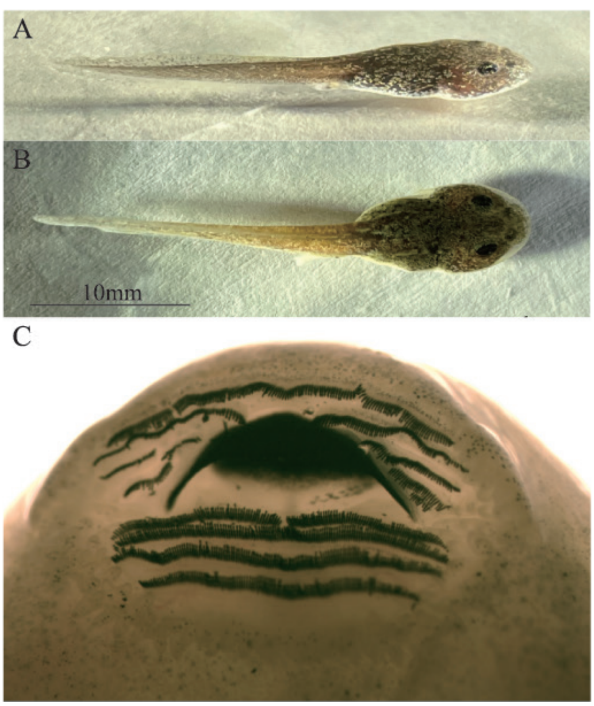

Figure 8 Tadpole of *Rana taihangensis* **sp. nov.** Lateral (A) and dorsal (B) views of a Gosner stage 35 individual in life. C: The structure of the mouth of a Gosner stage 40 individual in life.

is I: 3+3/III: 1+1 (Figure 8C). The papillae on the mouth angles around upper labium (the anterior corner of the mouth) and lower labium is in one row, with some additional tubercles at the angles of the mouth (Figure 8C).

Comparisons Within the *R. chensinensis* species group, *R. taihangensis* **sp. nov.** differs from *R. kukunoris* by having smaller size (in *R. taihangensis* **sp. nov.**, males SVL mean 44.9 mm, females mean 47.0 mm; in *R. kukunoris,* males SVL mean 56.3 mm, females mean 61.9 mm), longer hindlimbs 171% of SVL (versus 160% of SVL), tibio-tarsal articulation reaching to the anterior corner of eyes when leg stretched forward (versus tibio-tarsal articulation reaching to tympanum when leg stretched forward), relative finger lengths: III>IV>I>II (versus III>I>IV>II), two distinct nuptial pads with an obvious gap (versus four nuptial pads with a narrow gap) (Figure 9A), dorsal skin smooth (versus rough dorsum). The new species differs from *R. chensinensis* by having two distinct nuptial pads (versus four nuptial pads) (Figure 9B), hindlimbs 170% of SVL (versus 185% of SVL), head length 33% of SVL (versus 34% of SVL), lower arm diameter 8% of SVL (versus 9% of SVL), tibio-tarsal articulation reaching to the anterior corner of eyes when leg stretched forward (versus tibio-tarsal articulation reaching to nostrils or beyond tip of snout when leg stretched forward), toes two-thirds webbed (versus toes one half webbed). The new species differs from *R. huanrenensis* by having internal subgular vocal sacs (versus absent), the anterior edges of vomerine teeth in line with the center of the choanae (versus the vomerine teeth located behind the posterior level of the choanae), having two distinct nuptial pads (versus four nuptial pads) (Figure 9C), heels overlapping when limbs are held at right angles to body axis (versus heels just meeting when the limbs are folded at right angle to the body), foot length longer than tibia length (versus foot length shorter than tibia length), toes two-thirds webbed (versus toes nearly fully webbed). The new species differs from The new species differs from *R. dybowskii* by having smaller body size (in *R. taihangensis* **sp. nov.**, males SVL mean 44.9 mm, females mean 47.0 mm; in *R. dybowskii,* males SVL mean 62.6mm, females mean 67.1 mm), the tympanum diameter shorter than half of the eye diameter (TD/ED = 0.47) (versus the tympanum diameter larger than half of the eye diameter), hindlimbs 171% of SVL (versus 175% of SVL), tibio-tarsal articulation reaching to the anterior corner of eyes when leg stretched forward (versus tibio-tarsal articulation reaching to the anterior corner of eyes or nostrils when leg stretched forward), having two distinct nuptial pads with an obvious gap (versus four nuptial pads with a narrow gap) (Figure 9D), toes two-thirds webbed (versus toes nearly fully webbed). The new species differs from *R. huanrenensis* by having internal subgular vocal sacs (versus absent), the anterior edges of vomerine teeth in line with the center of the choanae (versus the vomerine teeth located behind the posterior level of the choanae), heels overlapping when limbs are held at right angles to body axis (versus heels just meeting when the limbs are folded at right angle to the body), foot length longer than tibia length (versus foot length shorter than tibia length), toes two-thirds webbed (versus toes nearly fully webbed).

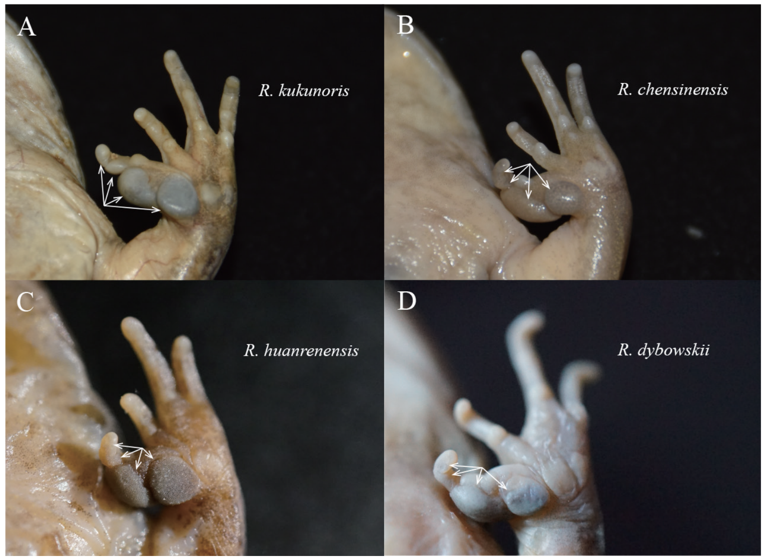

Figure 9 Male nuptial pads of *R. kukunoris* (QZ817) from Shiqu County, Sichuan Province, China (A), *R. chensinensis* (HNNU1604III002) from Xiaoqinling Mountain in Henan Province, China (B), *R. huanrensis* (39702) from Hulunbuir City, Inner Mongolia Autonomous Region, China (C), and *R. dybowskii* (94352) from Benxi City, Liaoning Province, China (D). More voucher information is presented in Supplementary Table S1.

4. Discussion

Because of the phenotypic plasticity and local morphological adaptations to the similar habitats, cryptic species are common in amphibians (Chen *et al*., 2020; Shen *et al*., 2020; Stuart *et al*., 2006). Recently, the integrative taxonomy of morphological comparisons and molecular analyses facilitated the identification of many cryptic amphibian species (Che *et al*., 2020; Shen *et al*., 2020; Shi *et al*., 2020; Shi *et al*., 2021; Wang *et al*., 2020). Phylogenetic and biogeographic analyses suggested the existence of cryptic species in the *R. chensinensis* species group (Zhou *et al*., 2012). In this study, through extensive sampling, two robust monophyletic subclades—subclade C and T—were revealed for the samples from the Taihang Mountains based on the phylogenetic analysis (BPP = 1.00). Subclade C included the haplotypes from the southwest of the Taihang Mountains (locality 15), the east Qinling Mountains (localities 16–17), and the haplotype of *R. chensinensis* from the type locality—the middle Qinling Mountains in Shaanxi Province. The pairwise divergence within subclade C was lower (0.2%), and based on the aforementioned evidence, subclade C should be *R. chensinensis* sensu stricto.

The highly supported subclade T comprised the haplotypes from the majority area of the Taihang Mountains (localities 1–14), and it has a close affinity with *R. kukunoris* (BPP = 1.00). The pairwise distance between subclade T and *R. kukunoris* (4.8%) is obviously higher than the divergence threshold of 3% for identifying amphibian cryptic species based on the standard mitochondrial barcoding marker (Chen *et al*., 2020). In addition, morphological differentiation confirmed the phylogenetic results, and both supported the validity of a new species (*R. taihangensis* **sp. nov.**) in the *R. chensinensis* species group. According to the sampling sites and the phylogenetic relationship between our study and that of Zhou *et al*. (2012), the new species (i.e., *R. taihangensis* **sp. nov.**) revealed in this study corresponds to the Clade L in the phylogenetic tree of the *R. chensinensis* species group in Zhou *et al*. (2012). Hence, we proposed that the populations formerly recorded as *R. chensinensis* in Beijing City, Hebei Province, and the southeastern Taihang Mountains of Henan Province (localities 1–14) should be revised to *R. taihangensis* **sp. nov.**, whereas the populations of the southwestern Taihang Mountains (locality 15), Xiaoqinling Mountains, and Funiu Mountains in Henan Province (localities 16–17, the eastern foothills of the Qinling Mountains) remain *R. chensinensis* sensu stricto.

Numerous phylogeographic studies have demonstrated that mountain ranges may generate geographic barriers and contribute to the speciation (Wang *et al*., 2016; Wiens *et al*., 2019; Xu *et al*., 2018; Yan *et al*., 2010). The dramatic uplift of the plateau and the associated climatic change of eastern Asia are considered as the major drivers of vicariant speciation for many organisms (Che *et al*., 2010; Wang *et al*., 2016; Wu *et al*., 2020). With the uplift of the Qinghai-Tibetan plateau (QTP), a cold and arid climate developed in the northeastern

QTP, and the three-stepped terrain formed in China. Furthermore, the uplifting of the Qinling Mountains formed the biogeographic boundary between southern and northern China (Rost 1994; Webb and Bartlein, 1992; Wu *et al.,* 2020; Zhou *et al*., 2012). The diversification of *R. taihangensis* **sp. nov.**, *R. chensinensis,* and *R. kukunoris* also indicated the effect of long-term geographic isolation and ecological divergence between species because of the orogeny of the QTP. The geographic distributions of *R. taihangensis* **sp. nov.**, *R. chensinensis* and *R. kukunoris* are primarily located in the Taihang Mountains, Qinling Mountains and the eastern edge of QTP boundaries, respectively, suggesting the role of mountain edges as a potential geographic barrier for their dispersal and divergence.

In addition, the riverine barrier hypothesis (reviewed in Chen *et al*., 2020) might explain the distribution patterns and genetic variation of *R. taihangensis* **sp. nov.** and *R. chensinensis*. In the southern Taihang Mountains, the distributions of *R. chensinensis* sensu stricto and *R. taihangensis* **sp. nov.** were separated by drainage. The populations of *R. chensinensis* sensu stricto are only distributed in the Yellow River Basin, whereas all the populations of *R. taihangensis* **sp. nov.** are located within the Haihe River system (Figure 1). The role of rivers in shaping the range boundaries and genetic structure of species has been investigated in a range of amphibian species (Chen *et al*., 2020; Li *et al*., 2009; Nowakowski *et al*., 2015; Wang *et al*., 2015; Yan *et al*., 2013; Zhang *et al*., 2010). Regarding the *R. chensinensis* group, barriers to gene flow produced by the complex topography of mountains and/or river systems might contribute to the high level of species diversity in northern and central China. In addition, considering the gene flow previously revealed between *R. chensinensis* and *R. kukunoris* (Qi *et al*., 2014; Zhou *et al*., 2012), it is also possible that gene exchange may occur during or after the speciation of the new species, particularly in populations at the periphery of its distribution range, which is a common mechanism underlying divergence (Smadja and Butlin, 2011). Further studies should be conducted to determine the detailed roles of the mountain ridges, river systems and gene flow in the diversification and distribution of the *Rana* species.

Acknowledgements We would like to thank Meihua ZHANG from the Chengdu Institute of Biology, Chinese Academy of Sciences for providing samples of *R. kukunoris* for morphological measurements. We are grateful to Yuxiao HE, Youqiang LU, Qiqi FENG, Dian LIU, Can KE, Yimin ZHANG, Shuxuan GAO, Yanjun ZHU, Yao LIU and Guilin HU for their efforts in the field surveys, Xuewei LI for work in measuring samples. This study was supported by the Biodiversity Survey and Assessment Project of the Ministry of Ecology and Environment, China (2019HJ2096001006), China Biodiversity Observation Networks (Sino BON), the National Natural Science Foundation of China (31872220, U21A20192 and 31572245), the Natural Science Foundation of Henan Province (202300410222) and the Second National Survey of Terrestrial Wildlife Resources Project of the National Forestry and Grassland Bureau of China.

References

AmphibiaChina. 2021. The database of Chinese amphibians. Kunming Institute of Zoology (CAS), Kunming, Yunnan, China. Electronic Database accessible: http://www.amphibiachina.org/

Che J., Pang J., Zhao E. M., Matsui M., Zhang Y. P. 2007. Phylogenetic relationships of the Chinese brown frogs (genus *Rana*) inferred from partial mitochondrial 12S and 16S rRNA gene sequences. Zoolog Sci, 24(1): 71–80

Che J., Jiang K., Zhang Y. P. 2020. Amphibians and Reptiles in Tibet—Diversity and Evolution. Beijing: Science Press (In Chinese)

Che J., Zhou W. W., Hu J. S., Yan F., Papenfuss T. J., Wake D. B., Zhang Y. P. 2010. Spiny frogs (Paini) illuminate the history of the Himalayan region and Southeast Asia. Proc Natl Acad Sci USA, 107(31):13765–13770

Chen Z., Li H. Y., Zhai X. F., Zhu Y. J. He Y. X., Wang Q. Y., Li Z., Jiang J. P., Xiong R. C., Chen X. H. 2020. Phylogeography, speciation and demographic history: Contrasting evidence from mitochondrial and nuclear markers of the *Odorrana graminea* sensu lato (Anura, Ranidae) in China. Mol Phyl Evol, 144: 106701

Fei L., Hu S. Q., Ye C. Y., Huang Y. Z. 2009. Fauna Sinica, Amphibia, Vol. Anura. Beijing: Science Press (In Chinese)

Fei L., Ye C. Y, Jiang J. P. 2010. Colored atlas of Chinese Amphibians. Chengdu: Sichuan Publishing House of Science and Technology (In Chinese)

Frost D. R. 2021. Amphibian species of the world 6.1, an online reference (9 November 2021). New York: American Museum of Natural History. available from URL: https:// amphibiansoftheworld.amnh.org/index.php

Huson D. H., Bryant D. 2006. Application of Phylogenetic Networks in Evolutionary Studies. Mol Biol Evol, 23(2): 254–267

Lanfear R., Frandsen P. B., Wright A. M., Senfeld T., Calcott B. 2016. PartitionFinder 2: New methods for selecting partitioned models of evolution for molecular and morphological phylogenetic analyses. Mol Biol Evol, 34(3): 772–773

Li P. P., Lu Y. Y., Li A. 2014. Taxonomy and Distribution of Chinese Brown frog, *Rana chensinensis*. J Snake, 26(2): 156–158 (In Chinese)

Li R., Chen W., Tu L., Fu J. 2009. Rivers as barriers for high elevation amphibians: a phylogeographic analysis of the alpine stream frog of the Hengduan Mountains. J Zool, 277(4): 309–316

Linnaeus C. 1758. Systema naturae per regna tria naturae, secundum classes, ordines, genera, species, cum characteribus, differentiis, synonymis, locis. Sweden: Stockholm, L. Salvii

Liu C. C., Hu S. Q. 1961. Chinese amphibians (Anura). Beijing: Science Press (In Chinese)

Nowakowski A. J., DeWoody J. A., Fagan M. E., Willoughby J. R., Donnelly M. A. 2015. Mechanistic insights into landscape genetic structure of two tropical amphibians using field-derived resistance surfaces. Mol Ecol, 24(3): 580–595

Qi Y., Lu B., Gao H. Y., Hu P., Fu J. Z. 2014. Hybridization and mitochondrial genome introgression between *Rana chensinensis* and *R. kukunoris*. Mol Ecol, 23(22):5575–5588

Qu W. Y., Lv J. Q., Zhang S. L. 1995. Amphibian fauna and zoogeographic

division of Henan Province. Sichuan J Zool, 107–110 (In Chinese)

R Development Core Team. 2010. R: A Language and Environment for Statistical Computing, Vienna: R Foundation for Statistical Computing

Ronquist F., Huelsenbeck J. P. 2003. MRBAYES 3: Bayesian phylogenetic inference under mixed models. Bioinformatics, 19(12): 1572–1574

Rost K. T. 1994. Paleoclimatic field studies in and along the Qinling Shan (Central China), Geo J, 34(1): 107–120

Rozas J., Sánchez-DelBarrio J. C., Messeguer X., Rozas R. 2003. DnaSP, DNA polymorphism analyses by the coalescent and other methods. Bioinformatics, 19: 2496–2497

Smadja C. M., Butlin R. K. 2011. A framework for comparing processes of speciation in the presence of gene flow. Mol Ecol, 20(24): 5123–5140

Shen H. J., Zhu Y. J., Li Z., Chen Z., Chen X. H. 2020. Reevaluation of the Holotype of *Odorrana schmackeri* Boettger, 1892 (Amphibia: Anura: Ranidae) and Characterization of One Cryptic Species in *O. schmackeri* sensu lato through Integrative Approaches. Asian Herpetol Res, 11(4): 297–311

Shi S. C., Li D. H., Zhu W. B., Jiang W., Jiang J. P., Wang B. 2021. Description of a new toad of *Megophrys* Kuhl, Van Hasselt, 1822 (Amphibia: Anura: Megophryidae) from western Yunnan Province, China. Zootaxa, 4942(3): 351–381

Shi S. C., Zhang M. H., Xie F., Jiang J. P., Liu W. L., Li D., Li L., Wang B. 2020. Multiple data revealed two new species of the Asian horned toad *Megophrys* Kuhl & Van Hasselt, 1822 (Anura, Megophryidae) from the eastern corner of the Himalayas. ZooKeys, 977: 101–161

Stuart B. L., Inger R. F., Voris H. K. 2006. High level of cryptic species diversity revealed by sympatric lineages of Southeast Asian forest frogs. Biol Lett, 2(3): 470–474

Tamura K., Stecher G., Peterson D., Filipski A., Kumar S. 2013. MEGA6: Molecular evolutionary genetics analysis, version 6.0. Mol Biol Evol, 30(12): 2725–2729

Tanaka-Ueno T., Matsui M., Sato T., Takenaka S., Takenaka O. 1998. Phylogenetic relationships of brown frogs with 24 chromosomes from Far East Russia and Hokkaido assessed by mitochondrial cytochrome *b* gene sequences (*Rana*: Ranidae). Zool Sci, 15(2): 289–294

Vaidya G., Lohman D. J., Meier R. 2011. Sequencematrix: Concatenation software for the fast assembly of multi-gene datasets with character set and codon information. Cladistics, 27(2): 171–180

Wan H., Lyu Z. T., Qi S., Zhao J., Li P. P., Wang Y. Y. 2020. A new species of the *Rana japonica* group (Anura, Ranidae, *Rana*) from China, with a taxonomic proposal for the *R. johnsi* group. ZooKeys, 942: 141–158

Wang B., Wu Y. Q., Peng J. W., Shi S. C., Lu N. N., Wu J. 2020. A new *Megophrys* Kuhl, Van Hasselt (Amphibia, Megophryidae) from southeastern China. ZooKeys, 904: 35–62

Wang G. L., Wu Y. H., Tang W. B., Hu Y., Bi M. C., Li S. W. 2019. Survey of amphibian and reptile resources in Taihang Mountainous of the Western Xingtai. Chinese J Zool, 54(3): 436–440 (In Chinese)

Wang H., Luo X., Meng S., Bei Y., Song T., Meng T., Li G., Zhang B. 2015. The phylogeography and population demography of the Yunnan Caecilian (*Ichthyophis bannanicus*): Massive Rivers as barriers to gene flow. PLoS One, 10(4): e0125770

Wang X., Gan X., Li J., Chen Y., He S. 2016. Cyprininae phylogeny revealedindependent origins of the Tibetan Plateau endemic polyploid cyprinids and their diversifications related to the Neogene uplift of the plateau. Sci China Life Sci, 59(11): 1149–1165

Webb T., Bartlein P. J. 1992. Global changes during the last 3 million years: climatic controls and biotic responses. Annu Rev Ecol Syst, 23(23): 141–173

Wiens J. J., Camacho A., Goldberg A., Jezkova T., Kaplan M. E., Lambert S. M., Miller E. C., Streicher J. W., Walls R. L. 2019. Climate change, extinction, and Sky Island biogeography in a montane lizard. Mol Ecol, 28(10): 2610–2624

Wu Y. F., Wu M. L., Cao Y. P. 2009. The fauna of Hebei, China: Amphibia, Reptilia and Mammalia. Hebei Shijiazhuang: Science and Technology Publishing House (In Chinese)

Wu H. H., Gu Q., Zhou C. J., Tang Y. T., Husemann M., Meng X. L., Zhang J. X., Nie G. X., Li X. J. 2020. Molecular phylogeny and biogeography of *Triplophysa* stone loaches in the Central Chinese Mountains. Biol J Linn Soc, 130(3): 563–577

Xia X. H., Xie Z., Salemi M., Chen L., Wang Y. 2003. An index of substitution saturation and its application. Mol Phyl Evol, 26(1): 1–7

Xie F., Ye C. Y., Fei L., Jiang J. P., Zeng X. M., Masafumi M. 1999. Taxonomic studies on brown frogs (*Rana*) from northeastern China (Amphibia: Ranidae). Zool Syst, 24(2): 224-231 (In Chinese)

Xie F., Ye C. Y., Fei L., Jiang J. P., Masafumi M. 2000. Taxonomical studies on the populations of *Rana chensinensis* in north-western China (Amphibia: Ranidae). Zool Syst, 25(2): 228-235 (In Chinese)

Xu X., Kuntner M., Liu F., Chen J., Li D. 2018. Formation of rivers and mountains drives diversification of primitively segmented spiders in continental East Asia. J Biogeogr, 45(9): 2080–2091

Yan F., Zhou W. W., Zhao H. T., Yuan Z. Y., Wang Y. Y., Jiang K., Jin J. Q., Murphy R. W., Che J., Zhang Y. P. 2013. Geological events play a larger role than Pleistocene climatic fluctuations in driving the genetic structure of *Quasipaa boulengeri* (Anura: Dicroglossidae). Mol Ecol, 22(4): 1120–1133

Yan J., Wang Q. X., Chang Q., Ji X., Zhou K. Y. 2010. The divergence of two independent lineages of an endemic Chinese gecko, *Gekko swinhonis*, launched by the Qinling orogenic belt. Mol Ecol, 19(12): 2490–2500

Yuan Z. Y., Zhou W. W., Chen X., Poyarkov N. A., Chen H. M., Jang-Liaw N. H., Chou W. H., Matzke N. J., Iizuka K., Min M. S., Kuzmin S. L., Zhang Y. P., Cannatella D. C., Hillis D. M., Che J. 2016. Spatiotemporal diversification of the true frogs (Genus *Rana*): A historical framework for a widely studied group of model organisms. Syst Biol, 65(5): 824–842

Zhang D. R., Chen M. Y., Murphy R. W., Che J., Pang J. F., Hu J. S., Luo J., Wu S. J., Ye H., Zhang Y. P. 2010. Genealogy and palaeodrainage basins in Yunnan Province: Phylogeography of the Yunnan spiny frog, *Nanorana yunnanensis* (Dicroglossidae). Mol Ecol, 19(18): 3406–3420

Zhou W. W., Wen Y., Fu J. Z., Xu Y. B., Jin J. Q., Ding L., Min M. S., Che J., Zhang Y. P. 2012. Speciation in the *Rana chensinensis* species complex and its relationship to the uplift of the Qinghai-Tibetan Plateau. Mol Ecol, 21(4): 960–973

Handling Editor: Heling Zhao

How to cite this article:

SHEN H. J., XU M. Y., YANG X. Y., CHEN Z., XIAO N. W., CHEN X. H. A New Brown Frog of the Genus *Rana* (Anura, Ranidae) from North China, with a Taxonomic Revision of the *R. chensinensis* Species Group. Asian Herpetol Res, 2022, 13(3): 145–158. DOI: 10.16373/j.cnki.ahr.210062

Appendix

Table S1 Samlpe information and sequences of three mitochondrial genes downloaded from GenBank. The file can be downloaded from the website https://pan.baidu.com/s/1NXZtWQKBrq7RptczljS3eg?pwd=g7go (access code: g7go).